17,09

Energy Spectrum and Optical Absorption Spectra of endohedral Fullerenes Lu_3NC_{80} and Y_3NC_{80} within the Hubbard Model

© A.V. Silant'ev

Mari State University,
Yoshkar-Ola, Russia

E-mail: kvvant@rambler.ru

Received September 27, 2021
Revised September 27, 2021
Accepted October 12, 2021

Anticommutator Green's functions and energy spectra of fullerene C_{80}, endohedral fullerenes $Lu_3N@C_{80}$ and $Y_3N@C_{80}$ with the Ih symmetry groups have been obtained in an analytical form within the Hubbard model and static fluctuation approximation. The energy states have been classified using the methods of group theory, and the allowed transitions in the energy spectra of molecules C_{80}, $Lu_3N@C_{80}$ and $Y_3N@C_{80}$ have been determined. On the basis of these spectra, an interpretation of experimentally observed optical absorption bands endohedral fullerenes $Lu_3N@C_{80}$ and $Y_3N@C_{80}$.

Keywords: Hubbard model, Green's functions, energy spectrum, nanosystems, fullerene C_{80}, endohedral fullerene $Lu_3N@C_{80}$, endohedral fullerene $Y_3N@C_{80}$.

DOI: 10.21883/PSS.2022.02.53979.213

1. Introduction

Both physical and chemical properties of fullerenes have been studied extensively since the discovery of these molecules in 1985 [1]. The examination of a wide range of fullerenes revealed that those following the isolated pentagon rule [2] are the most stable. In addition, it was found that certain fullerenes following the isolated pentagon rule are unstable molecules that become stable following the penetration of atoms or molecules inside the carbon shell. Fullerene C_{80} with symmetry group I_h is one such molecule that the researchers failed to isolate in its hollow form (i.e., without atoms or molecules inside). The studies of endohedral fullerenes $M@C_{80}$ with symmetry group I_h (e.g., $Tm_3@C_{80}$ [3], $Dy_3N@C_{80}$ [4], $Lu_3N@C_{80}$ [5], $Y_3N@C_{80}$ [6]) showed that these molecules are stable.

Fullerene C_{80} consists of 12 pentagons and 30 hexagons and contains 80 carbon atoms (out of which 31924 isomers of C_{80} can be constructed). It was found that only seven isomers of fullerene C_{80} feature isolated pentagons: $C_{80}(I_h)$, $C_{80}(C_{2v})$, $C_{80}(C_{2v'})$, $C_{80}(D_{5h})$, $C_{80}(D_{5d})$, $C_{80}(D_2)$, and $C_{80}(D_3)$ [7]. Fullerene C_{80} with symmetry group I_h (see Fig. 1) is the one of them that attracts special attention. Just as fullerene C_{60}, this isomer of C_{80} has the highest symmetry of a truncated icosahedron I_h. The Schlegel diagram in Fig. 1 demonstrates that fullerene C_{80} with symmetry group I_h contains two groups of nonequivalent bonds. One of them is formed by bonds at the boundary between a hexagon and a pentagon, and equivalent bonds from the other group are located at the boundary between two hexagons. It is also seen from the Schlegel diagram that this isomer of fullerene C_{80} has two groups of nonequivalent carbon atoms: one group is formed by atoms located at pentagon vertices, and equivalent atoms from the other group are located at vertices where three hexagons meet. Note that all carbon atoms in fullerene C_{60} are equivalent, while bonds are, just as in C_{80}, divided into two groups. A considerable number of studies focused on the properties of fullerene C_{80} have already been published [3–6,8–10].

The Hubbard model [11] is commonly used to characterize the electronic properties of carbon fullerenes and nanotubes. It has been applied in the studies of electronic and optical properties of various carbon nanosystems [12–20]. For example, the Hubbard model in the approximation of static fluctuations was used to obtain the energy spectra and optical absorption spectra of fullerene C_{20} with symmetry groups I_h, D_{5d}, and D_{3d} [12]; fullerene C_{24} with symmetry groups O_h, D_6, and D_{6d} [13]; fullerene C_{26} with symmetry group D_{3h} [14]; fullerene C_{28} with symmetry group T_d [15]; fullerene C_{36} with symmetry group D_{6h} [16]; fullerene C_{60} [17]; and fullerene C_{70} [18]. The authors of [19] used it to determine the electronic properties of carbon nanotubes. The results obtained in [17,18] agree fairly well with experimental data.

The aim of this study is to examine the energy spectra of endohedral fullerenes $Lu_3N@C_{80}$ and $Y_3N@C_{80}$ within the Hubbard model in the static fluctuation approximation (SFA). It was found experimentally [5,6] that the molecules of endohedral fullerenes $Lu_3N@C_{80}$ and $Y_3N@C_{80}$ have symmetry group I_h. Endohedral fullerenes $Lu_3N@C_{80}$ and $Y_3N@C_{80}$ are formed when molecules Lu_3N and Y_3N penetrate inside fullerene C_{80}. It is assumed that the introduction of metal atoms and molecules into a fullerene does not alter its energy levels in any significant way. Therefore, it may be assumed as a first approximation that an embedded molecule only adds excess electrons to the fullerene core [21]. Thus, to prepare for the study of the energy spectra of molecules $Lu_3N@C_{80}$ and $Y_3N@C_{80}$, we

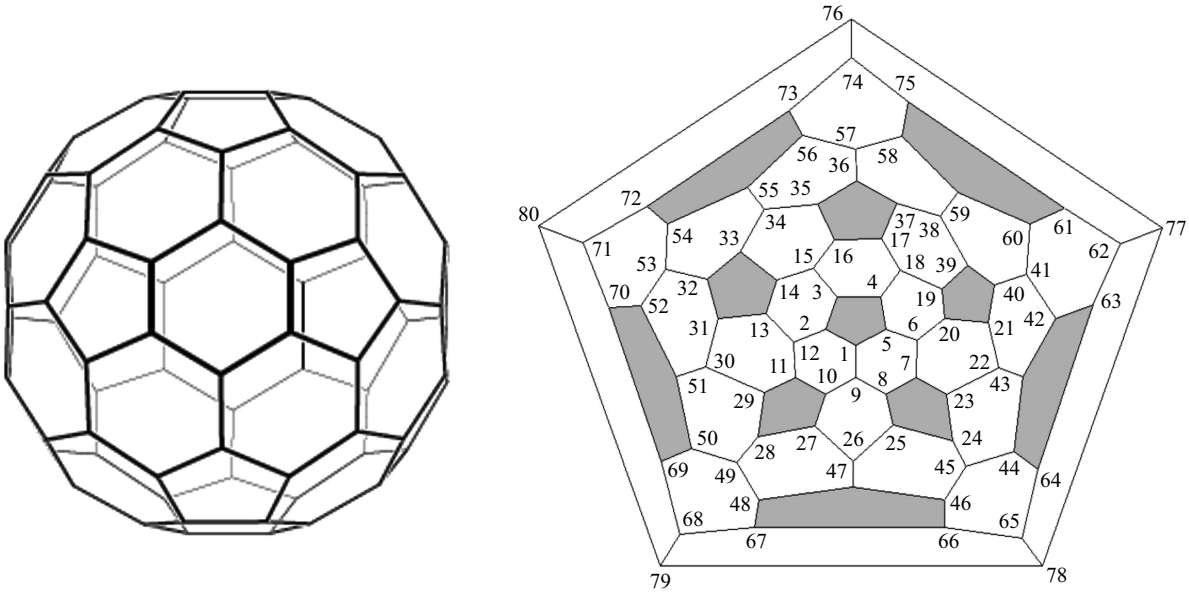

Figure 1. Fullerene C_{80} with symmetry group I_h and its Schlegel diagram showing the position of carbon atoms, bonds between carbon atoms, and pentagons.

first examine the energy spectrum of fullerene C_{80} with symmetry group I_h.

2. Energy spectrum of fullerene C_{80}

We use the Hubbard model [11] to characterize the π-electron system of fullerene C_{80}:

$$H = \sum_{\sigma,i} \varepsilon_i n_{I\sigma} + \sum_{\sigma,i\neq j} t_{ij} c^+_{i\sigma} c_{j\sigma} + \frac{1}{2}\sum_{\sigma,i} U_i n_{i\sigma} n_{i\bar{\sigma}}, \qquad (1)$$

where $c^+_{i\sigma}$, $c_{i\sigma}$ are the operators of creation and annihilation of electrons with spin σ at site i; $n_{i\sigma}$ is the operator of the number of particles with spin σ at site i; ε_i is the energy of the one-electron atomic state at site i; t_{ij} is the transfer integral characterizing electron hops from site i to site j; U_i is the energy of Coulomb repulsion of two electrons located at site i; and $\bar{\sigma} = -\sigma$.

Using Hamiltonian (1) and the Schlegel diagram shown in Fig. 1, we write the equations of motion in SFA [20] for all creation operators $c^+_{f\sigma}(\tau)$ in the Heisenberg representation:

$$\begin{cases} \frac{dc^+_{1\sigma}}{d\tau} = \varepsilon \cdot c^+_{1\sigma} + t(c^+_{2\sigma} + c^+_{5\sigma}) + t_1 c^+_{9\sigma} + U \cdot c^+_{1\sigma} n_{1\bar{\sigma}} \\ \frac{d(c^+_{1\sigma} n_{1\bar{\sigma}})}{d\tau} = (\varepsilon + U) \cdot c^+_{1\sigma} n_{1\bar{\sigma}} \\ \qquad + t(c^+_{2\sigma} n_{2\bar{\sigma}} + c^+_{5\bar{\sigma}} n_{5\bar{\sigma}}) + t_1 c^+_{9\sigma} n_{9\bar{\sigma}} \\ \ldots\ldots\ldots\ldots\ldots\ldots\ldots\ldots\ldots\ldots\ldots\ldots\ldots\ldots \\ \frac{dc^+_{80\sigma}}{d\tau} = \varepsilon \cdot c^+_{80\sigma} + t(c^+_{76\sigma} + c^+_{79\sigma}) + t_1 c^+_{71i\sigma} + U \cdot c^+_{80\sigma} n_{80\bar{\sigma}} \\ \frac{d(c^+_{80\sigma} n_{80\bar{\sigma}})}{d\tau} = (\varepsilon + U) \cdot c^+_{80\sigma} n_{80\bar{\sigma}} \\ \qquad + t(c^+_{76\sigma} n_{76\bar{\sigma}} + c^+_{79\bar{\sigma}} n_{79\bar{\sigma}}) + t_1 c^+_{71\sigma} n_{71\bar{\sigma}} \end{cases}, \qquad (2)$$

where t is the transfer integral characterizing electron hops from site i to site j if the segment connecting these sites is the boundary between a hexagon and a pentagon; t_1 is the transfer integral characterizing electron hops from site i to site j if the segment connecting these sites is the boundary between two hexagons.

Using the solution of system (2), we find the Fourier transforms of anticommutator Green's functions:

$$\left\langle \langle c^+_{j\sigma} | c_{j\sigma} \rangle \right\rangle = \frac{i}{2\pi} \sum_{m=1}^{40} \frac{F_{j,m}}{E - E_m + ih}, \qquad (3)$$

$$E_k = \varepsilon + e_k, \; E_{k+20} = E_k + U, \; F_{j,k} = q_k Q_{j,k},$$

$$Q_{j,k+20} = Q_{j,k}, \quad k = 1 \ldots 20,$$

$$q_k = \begin{cases} 1 - \frac{n}{2}, & k = 1 \ldots 20 \\ \frac{n}{2}, & k = 21 \ldots 40 \end{cases}, \quad h \to 0,$$

where

$$Q_{1,1} = -\frac{e_1}{120\sqrt{t^2 + 3t_1^2}},$$

$$Q_{1,m} = -\frac{1}{20}\Big[4e_m^5 + 18t_1^4 e_m - 9te_m^4 + 36t_1^2 te_m^2 - 2t^2 e_m^3 - 27tt_1^4 - 18t_1^2 e_m^3 - 10t^2 t_1^2 e_m + 8t^3 e_m^2\Big]\Big[8t^4 e_m - 24t^3 e_m^2 + 4t^3 t_1^2 + 4t^2 e_m^3 + 20t^2 t_1^2 e_m + 15te_m^4 - 54tt_1^2 e_m^2 + 27tt_1^4 - 6e_m^5 + 24t_1^2 e_m^3 - 18t_1^4 e_m\Big]^{-1}, \; m = 2, 5, 8, 9, 15, 20;$$

$$Q_{1,m} = -\frac{2te_m^2 + 3t^2 e_m - tt_1^2 + 6t_1^2 e_m - 3e_m^3}{12(2t^3 + tt_1^2 - 6(t^2 + t_1^2)e_m - 3te_m^2 + 4e_m^3)}, \quad m = 3, 7, 13, 17;$$

$$Q_{1,m} = -\frac{2e_m^2 - 3t_1^2 + te_m}{15(t^2 + 3t_1^2 - 2te_m - 3e_m^2)},$$

$$m = 4, 6, 11, 12, 18, 19;$$

$$Q_{1,10} = Q_{1,16} = \frac{2}{15},$$

$$Q_{1,14} = \frac{e_{14}}{120\sqrt{t^2 + 3t_1^2}},$$

$$Q_{2,1} = 3Q_{1,14},$$

$$Q_{2,m} = -\frac{3}{10}(e_m - 2t)(e_m^4 - te_m^3 - 3(t_1^2 + t^2)e_m^2 + 2t^3e_m + 3tt_1^2e_m + t^2t_1^2)\Big[8t^4e_m - 24t^3e_m^2 + 4t^3t_1^2 + 4t^2e_m^3 + 20t^2t_1^2e_m + 15te_m^4 - 54tt_1^2e_m^2 + 27tt_1^4 - 6e_m^5 + 24t_1^2e_m^3 - 18t_1^4e_m\Big]^{-1},\ m = 2, 5, 8, 9, 15, 20;$$

$$Q_{2,m} = \frac{(e_m - 2t)(-t^2 + e_m^2 + te_m)}{4(2t^3 + tt_1^2 - 6(t^2 + t_1^2)e_m - 3te_m^2 + 4e_m^3)},$$

$$m = 3, 7, 13, 17;$$

$$Q_{2,m} = -\frac{-t^2 + e_m^2 + te_m}{5(t^2 + 3t_1^2 - 2te_m - 3e_m^2)},$$

$$m = 4, 6, 11, 12, 18, 19;$$

$$Q_{2,10} = Q_{2,16} = 0,$$

$$Q_{2,14} = 3Q_{1,1}, \qquad (4)$$

$$e_1 = t - \sqrt{t^2 + 3t_1^2},$$

$$e_2 = x_1,$$

$$e_3 = \frac{1}{4}\left(t - (9t^2 + 8t_1^2 + 4z)^{1/2} - \sqrt{\begin{matrix}2\big(9t^2 + 8t_1^2 - 2z - t(9t^2 + 8t_1^2 + 4z)^{1/2} \\ - 4((z - t_1^2 - t^2)^2 - 28t^2t_1^2)^{1/2}\big)\end{matrix}}\right),$$

$$e_4 = -\frac{2}{3}\sqrt{4t^2 + 9t_1^2}\cos\left(\frac{\varphi_2}{3}\right) - \frac{t}{3},$$

$$e_5 = x_2,$$

$$e_6 = -\frac{2}{3}\sqrt{4t^2 + 9t_1^2}\cos\left(\frac{\varphi_1}{3}\right) - \frac{t}{3},$$

$$e_7 = \frac{1}{4}\left(t + (9t^2 + 8t_1^2 + 4z)^{1/2} - \sqrt{\begin{matrix}2\big(9t^2 + 8t_1^2 - 2z + t(9t^2 + 8t_1^2 + 4z)^{1/2} \\ + 4((z - t_1^2 - t^2)^2 - 28t^2t_1^2)^{1/2}\big)\end{matrix}}\right),$$

$$e_8 = x_3,$$

$$e_9 = x_4,$$

$$e_{10} = (-1 + \sqrt{5})t/2,$$

$$e_{11} = \frac{2}{3}\sqrt{4t^2 + 9t_1^2}\cos\left(\frac{\varphi_1}{3} + \frac{\pi}{3}\right) - \frac{t}{3},$$

$$e_{12} = \frac{2}{3}\sqrt{4t^2 + 9t_1^2}\cos\left(\frac{\varphi_2}{3} + \frac{\pi}{3}\right) - \frac{t}{3},$$

$$e_{13} = \frac{1}{4}\left(t + (9t^2 + 8t_1^2 + 4z)^{1/2} + \sqrt{\begin{matrix}2\big(9t^2 + 8t_1^2 - 2z + t(9t^2 + 8t_1^2 + 4z)^{1/2} \\ + 4((z - t_1^2 - t^2)^2 - 28t^2t_1^2)^{1/2}\big)\end{matrix}}\right),$$

$$e_{14} = t + \sqrt{t^2 + 3t_1^2},$$

$$e_{15} = x_5,$$

$$e_{16} = -(1 + \sqrt{5})t/2,$$

$$e_{17} = \frac{1}{4}\left(t - (9t^2 + 8t_1^2 + 4z)^{1/2} + \sqrt{\begin{matrix}2\big(9t^2 + 8t_1^2 - 2z - t(9t^2 + 8t_1^2 + 4z)^{1/2} \\ - 4((z - t_1^2 - t^2)^2 - 28t^2t_1^2)^{1/2}\big)\end{matrix}}\right),$$

$$e_{18} = \frac{2}{3}\sqrt{4t^2 + 9t_1^2}\sin\left(\frac{\varphi_2}{3} + \frac{\pi}{6}\right) - \frac{t}{3},$$

$$e_{19} = \frac{2}{3}\sqrt{4t^2 + 9t_1^2}\cos\left(\frac{\varphi_1}{3} - \frac{\pi}{3}\right) - \frac{t}{3},$$

$$e_{20} = x_6,$$

$$z = \frac{2}{\sqrt{3}}\sqrt{3t_1^4 + 35t^2t_1^2 + 5t^4}\cos\left(\frac{\varphi_3}{3}\right),$$

$$\varphi_1 = \arccos\left(\frac{t(11t^2 + 54t_1^2)}{2(4t^2 + 9t_1^2)^{3/2}}\right),$$

$$\varphi_2 = \arccos\left(\frac{t(11t^2 - 54t_1^2)}{2(4t^2 + 9t_1^2)^{3/2}}\right),$$

$$\varphi_3 = \arccos\left(\frac{3^{3/2}t_1^2(29t^4 - t_1^4 + 25t^2t_1^2)}{(5t^4 + 35t^2t_1^2 + 3t_1^4)^{3/2}}\right). \qquad (5)$$

Here, $x_1, x_2, x_3, x_4, x_5, x_6$ are the roots of the following equation:

$$x^6 - 3tx^5 - (t^2 + 6t_1^2)x^4 + 2t(4t^2 + 9t_1^2)x^3 + (9t_1^4 - 4t^4 - 10t^2t_1^2)x^2 - tt_1^2(4t^2 + 27t_1^2)x + 19t^2t_1^4 = 0. \qquad (6)$$

As is known, poles of the Green's function characterize the energy spectrum of a quantum system [22]. Therefore, the energy spectrum of fullerene C_{80} with symmetry group I_h is defined by the values of E_m found in Green's

function (3). It can be seen from relation (3) that E_m may be presented in the following form:

$$E_k = \varepsilon + \frac{U}{2} + \bar{e_k}, \tag{7}$$

where $\bar{e_k}$ is the energy of the k-th level relative to energy $\varepsilon + U/2$:

$$\bar{e_k} = \begin{cases} e_k - \frac{U}{2}, & k = 1 \ldots 20 \\ e_k + \frac{U}{2}, & k = 21 \ldots 40 \end{cases}. \tag{8}$$

It can be seen from relations (7) and (8) that the energy states of fullerene C_{80} form two Hubbard subbands. The energy states forming the lower Hubbard subband are concentrated near energy $\bar{\epsilon}$, while the energy states forming the upper Hubbard subband are concentrated around $\varepsilon + U$.

The energy states forming the energy spectrum of fullerene C_{80} with symmetry group I_h may be classified according to irreducible representations of group I_h, which has the following representations of this kind: a_g, t_{1g}, t_{2g}, g_g, h_g, a_{1u}, t_{1u}, t_{2u}, g_u, h_u [23]. It can be shown that the energy states of fullerene C_{80} with symmetry group I_h are related to the irreducible representations of this group in the following way: $E_1(a_g)$, $E_2(t_{1u})$, $E_3(h_g)$, $E_4(g_u)$, $E_5(t_{2u})$, $E_6(g_g)$, $E_7(h_g)$, $E_8(t_{2u})$, $E_9(t_{1u})$, $E_{10,1}(h_u)$, $E_{10,2}(t_{1g})$, $E_{11}(g_g)$, $E_{12}(g_u)$, $E_{13}(h_g)$, $E_{14}(a_g)$, $E_{15}(t_{1u})$, $E_{16,1}(h_u)$, $E_{16,2}(t_{2g})$, $E_{17}(h_g)$, $E_{18}(g_u)$, $E_{19}(g_g)$, $E_{20}(t_{2u})$, $E_{21}(a_g)$, $E_{22}(t_{1u})$, $E_{23}(h_g)$, $E_{24}(g_u)$, $E_{25}(t_{2u})$, $E_{26}(g_g)$, $E_{27}(h_g)$, $E_{28}(t_{2u})$, $E_{29}(t_{1u})$, $E_{30,1}(h_u)$, $E_{30,2}(t_{1g})$, $E_{31}(g_g)$, $E_{32}(g_u)$, $E_{33}(h_g)$, $E_{34}(a_g)$, $E_{35}(t_{1u})$, $E_{36,1}(h_u)$, $E_{36,2}(t_{2g})$, $E_{37}(h_g)$, $E_{38}(g_u)$, $E_{39}(g_g)$, $E_{40}(t_{2u})$.

Each level of the energy spectrum of a quantum system is characterized by a degree of degeneracy, which may be determined using relation [17,18]

$$g_i = \sum_{j=1}^{N} Q_{j,i}, \tag{9}$$

where N is the number of sites in the nanosystem.

Inserting the expressions for $Q_{j,i}$ from (4) into formula (9), we find the numerical values for the degrees of degeneracy of the energy levels of fullerene C_{80} with symmetry group I_h:

$$g_1 = g_{14} = g_{21} = g_{34} = 1,$$

$$g_2 = g_5 = g_8 = g_9 = g_{15} = g_{20} = g_{22} = g_{25} = g_{28} = g_{29} = g_{35} = g_{40} = 3,$$

$$g_4 = g_6 = g_{11} = g_{12} = g_{18} = g_{19} = g_{24} = g_{26} = g_{31} = g_{32} = g_{38} = g_{39} = 4,$$

$$g_3 = g_7 = g_{13} = g_{17} = g_{23} = g_{27} = g_{33} = g_{37} = 5,$$

$$g_{10} = g_{16} = g_{30} = g_{36} = 8. \tag{10}$$

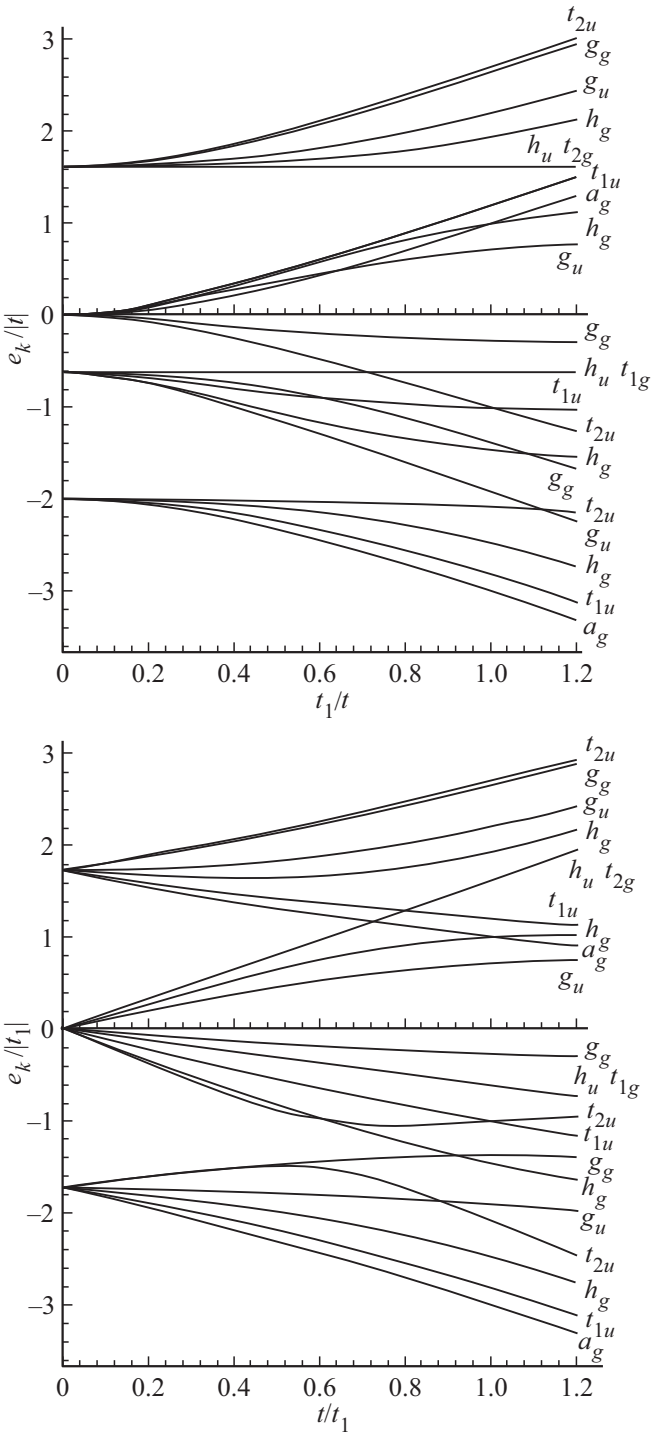

Figure 2. Dependence of parameters e_i on hopping integrals t and t_1.

Relations (7), (8), and (5) reveal the following features of the energy spectrum of fullerene C_{80}. It follows from the Schlegel diagram in Fig. 1 that the energy spectrum of fullerene C_{80} transforms at $t_1 = 0$ into the energy spectrum of a pentagon and an isolated atom; at $t = 0$, the energy spectrum of C_{80} transforms into the spectrum of a quantum system consisting of a single atom bound

Table 1. Energy spectrum of fullerene $Lu_3N@C_{80}$ with symmetry group I_h: energies of levels, degrees of their degeneracy, and irreducible representations of group I_h to which they belong

№	e_j, eV	E_j, eV	g_j	$E(\Gamma_j)$	№	e_j, eV	E_j, eV	g_j	$E(\Gamma_j)$
1	−4.993	−9.986	1	$E_1(a_g)$	21	0.669	−4.324	1	$E_{21}(a_g)$
2	−4.861	−9.854	3	$E_2(t_{1u})$	22	0.801	−4.192	3	$E_{22}(t_{1u})$
3	−4.612	−9.605	5	$E_3(h_g)$	23	1.050	−3.943	5	$E_{23}(h_g)$
4	−4.320	−9.313	3	$E_5(t_{2u})$	24	1.342	−3.651	3	$E_{25}(t_{2u})$
5	−4.218	−9.211	4	$E_4(g_u)$	25	1.444	−3.549	4	$E_{24}(g_u)$
6	−3.881	−8.874	5	$E_7(h_g)$	26	1.781	−3.212	5	$E_{27}(h_g)$
7	−3.833	−8.826	4	$E_6(g_g)$	27	1.829	−3.164	4	$E_{26}(g_g)$
8	−3.562	−8.555	3	$E_8(t_{2u})$	28	2.100	−2.893	3	$E_{28}(t_{2u})$
9	−3.547	−8.540	3	$E_9(t_{1u})$	29	2.115	−2.878	3	$E_{29}(t_{1u})$
10	−3.272	−8.265	5+3	$E_{10,1}(h_u), E_{10,2}(t_{1g})$	30	2.390	−2.603	5+3	$E_{30,1}(h_u), E_{30,2}(t_{1g})$
11	−3.028	−8.021	4	$E_{11}(g_g)$	31	2.634	−2.359	4	$E_{31}(g_g)$
12	−2.316	−7.309	4	$E_{12}(g_u)$	32	3.346	−1.647	4	$E_{32}(g_u)$
13	−2.107	−7.100	5	$E_{13}(h_g)$	33	3.555	−1.438	5	$E_{33}(h_g)$
14	−2.097	−7.090	1	$E_{14}(a_g)$	34	3.565	−1.428	1	$E_{34}(a_g)$
15	−1.953	−6.946	3	$E_{15}(t_{1u})$	35	3.709	−1.284	3	$E_{35}(t_{1u})$
16	−1.676	−6.669	5+3	$E_{16,1}(h_u), E_{16,2}(t_{2g})$	36	3.986	−1.007	5+3	$E_{36,1}(h_u), E_{36,2}(t_{2g})$
17	−1.437	−6.430	5	$E_{17}(h_g)$	37	4.225	−0.768	5	$E_{37}(h_g)$
18	−1.246	−6.239	4	$E_{18}(g_u)$	38	4.416	−0.577	4	$E_{38}(g_u)$
19	−0.918	−5.911	4	$E_{19}(g_g)$	39	4.744	−0.249	4	$E_{39}(g_g)$
20	−0.883	−5.876	3	$E_{20}(t_{2u})$	40	4.779	−0.214	3	$E_{40}(t_{2u})$

with another three isolated atoms. Relations (5) and Fig. 2 demonstrate that accidental degeneracy of certain energy levels occurs in fullerene C_{80} at certain values of the transfer integrals. In addition, the spectrum of fullerene C_{80} in Fig. 2 reveals accidental degeneracy of energy levels ($E_{10,1}(h_u)$ and $E_{10,2}(t_{1g})$; $E_{16,1}(h_u)$ and $E_{16,2}(t_{2g})$; $E_{30,1}(h_u)$ and $E_{30,2}(t_{1g})$; $E_{36,1}(h_u)$ and $E_{36,2}(t_{2g})$) that is not lifted when the transfer integrals change.

Thus, the energy spectrum of fullerene C_{80} with symmetry group I_h is characterized by relations (5), (7), (8), (9), and (10) within the Hubbard model in SFA.

3. Discussion

Let us consider the energy spectra of endohedral fullerenes $Lu_3N@C_{80}$ and $Y_3N@C_{80}$ that, as was demonstrated in [5,6], have symmetry group I_h.

The study of endohedral fullerene $Lu_3N@C_{80}$ [5] revealed that the distances between carbon atoms in this molecule are as follows:

$$x_{1,2} = 1.438\,\text{Å}, \quad x_{1,9} = 1.427\,\text{Å}. \tag{11}$$

We use the following relation to determine the numerical values of the transfer integrals corresponding to endohedral fullerene $Lu_3N@C_{80}$ [12,18]:

$$t_s = -8.17065\exp(-1.69521x_s). \tag{12}$$

It follows from relations (11) and (12) that the numerical values of the transfer integrals for endohedral fullerene $Lu_3N@C_{80}$ with symmetry group I_h are

$$t = t_{1,2} = -0.714\,\text{eV}, \quad t_1 = t_{1,9} = -0.727\,\text{eV}. \tag{13}$$

Relations (7) and (8) indicate that the numerical values of parameters ε and U are needed to construct the energy spectrum of endohedral fullerene $Lu_3N@C_{80}$. The required values ($\varepsilon = -7.824\,\text{eV}$, $U = 5.662\,\text{eV}$) were determined in [17] based on the experimentally measured optical absorption spectrum of fullerene C_{60} within the Hubbard model in SFA. Note that $U = 5.662\,\text{eV}$ agrees with the results presented in [24], where $U \sim 5\,\text{eV}$ was obtained. Inserting ε, U, t and t_1 from (13) into relations (7), (8), (5), and (6), we find the numerical values of $\bar{e_k}, E_k$ for endohedral fullerene $Lu_3N@C_{80}$. These values are listed in Table 1, and the energy spectrum of endohedral fullerene $Lu_3N@C_{80}$ is shown in Fig. 3.

Let us now consider the electronic structure of endohedral fullerene $Lu_3N@C_{80}$. It is assumed that the introduction of a molecule into a fullerene does not alter its energy levels in any significant way [21]. Therefore, it may be assumed as a first approximation that an embedded Lu_3N molecule only adds its four valence electrons to the core of fullerene C_{80}. Since the lower Hubbard subband is occupied completely by π electrons of fullerene C_{80}, four valence electrons of a Lu_3N molecule occupy (see Fig. 3) energy levels $E_{21}(a_g)$ and $E_{22}(t_{1u})$ in the upper Hubbard subband.

Let us now examine the energy spectrum of endohedral fullerene $Y_3N@C_{80}$. The study performed in [25] showed that the distances between carbon atoms in endohedral

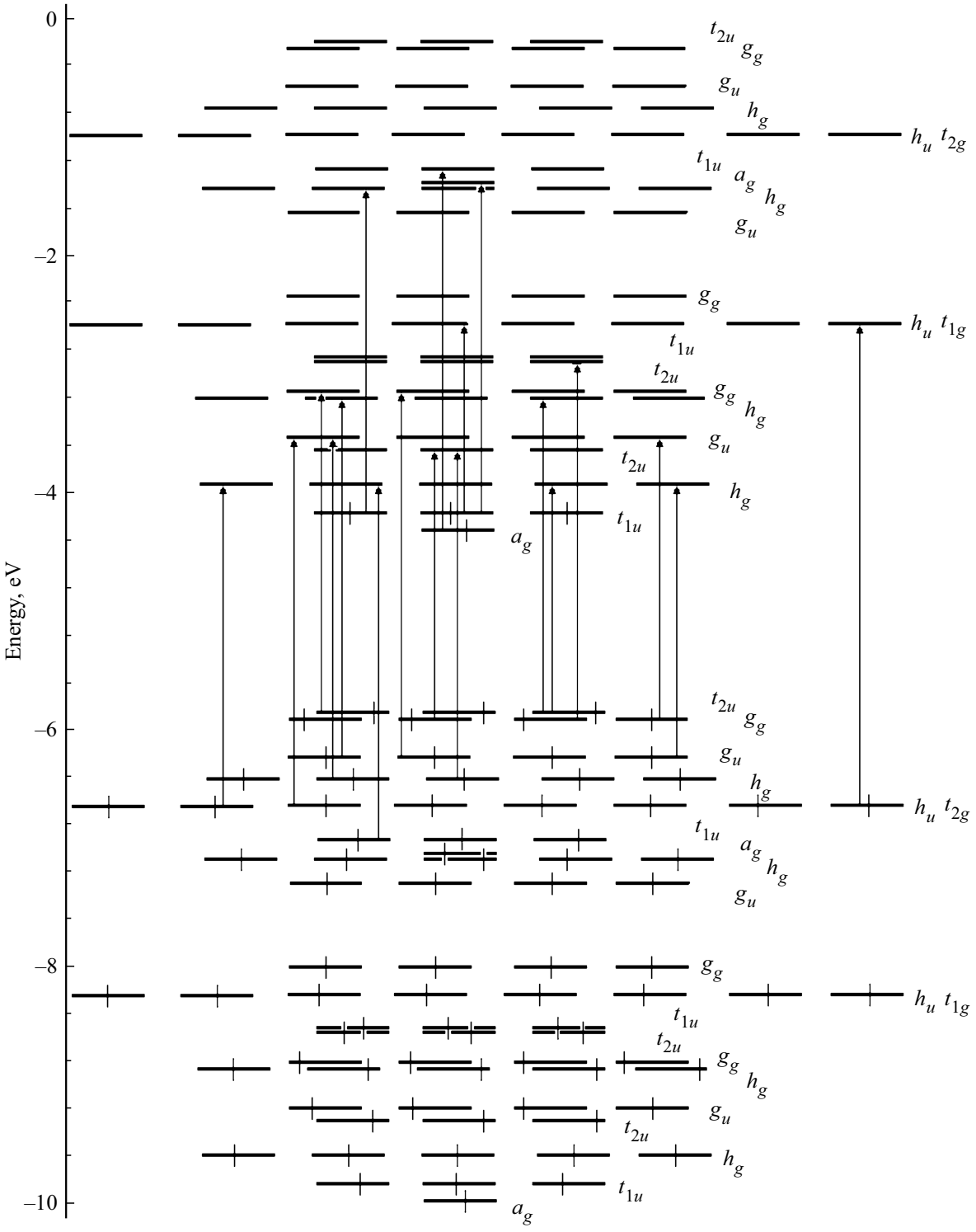

Figure 3. Energy spectrum of fullerene $Lu_3N@C_{80}$ with symmetry group I_h.

fullerene $Y_3N@C_{80}$ are

$$x_{1,2} = 1.45\,\text{Å}, \quad x_{1,9} = 1,45\,\text{Å}. \tag{14}$$

It follows from relations (12) and (14) that the numerical values of the transfer integrals for endohedral fullerene $Y_3N@C_{80}$ with symmetry group I_h are

$$t = t_{1,2} = -0.699\,\text{eV}, \quad t_1 = t_{1,9} = -0.699\,\text{eV}. \tag{15}$$

Inserting ε, U, t and t_1 from (15) into relations (7), (8), (5), and (6), we find the numerical values of $\bar{e_k}, E_k$ for endohedral fullerene $Y_3N@C_{80}$. These values

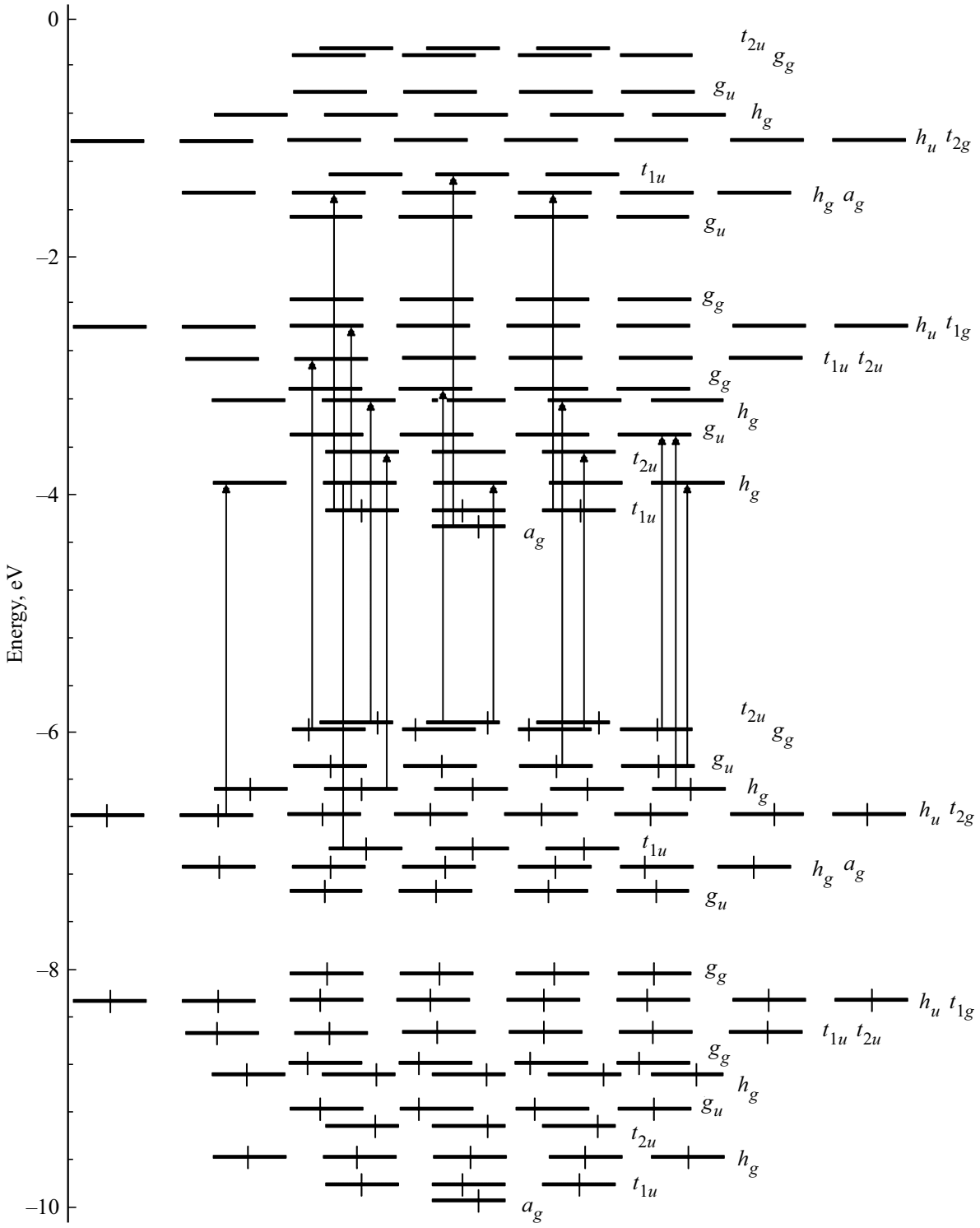

Figure 4. Energy spectrum of fullerene $Y_3N@C_{80}$ with symmetry group I_h.

are listed in Table 2, and the energy spectrum of endohedral fullerene $Y_3N@C_{80}$ is shown in Fig. 4. When a Y_3N molecule is introduced into fullerene C_{80}, four valence electrons of this molecule are, just as in the case of Lu_3N, added to the core of fullerene C_{80} and occupy energy levels $E_{21}(a_g)$ and $E_{22}(t_{1u})$ (see Fig. 4). It can be seen from Figs. 3, 4 and Tables 1 and 2 that energy levels $E_8(t_{2u})$ and $E_9(t_{1u})$, $E_{13}(h_g)$ and $E_{14}(a_g)$, $E_{28}(t_{2u})$ and $E_{29}(t_{1u})$, $E_{34}(h_g)$ and $E_{35}(a_g)$ of endohedral fullerene $Y_3N@C_{80}$ become, in contrast to what was found for $Lu_3N@C_{80}$, degenerate. This is attributable to the fact that two transfer integrals of the $Y_3N@C_{80}$ molecule are the same (see Fig. 2).

Table 2. Energy spectrum of fullerene $Y_3N@C_{80}$ with symmetry group I_h: energies of levels, degrees of their degeneracy, and irreducible representations of group I_h to which they belong

№	e_j, eV	E_j, eV	g_j	$E(\Gamma_j)$	№	e_j, eV	E_j, eV	g_j	$E(\Gamma_j)$
1	−4.929	−9.922	1	$E_1(a_g)$	21	0.733	−4.260	1	$E_{21}(a_g)$
2	−4.802	−9.795	3	$E_2(t_{1u})$	22	0.860	−4.133	3	$E_{22}(t_{1u})$
3	−4.561	−9.554	5	$E_3(h_g)$	23	1.101	−3.892	5	$E_{23}(h_g)$
4	−4.287	−9.280	3	$E_5(t_{2u})$	24	1.375	−3.619	3	$E_{25}(t_{2u})$
5	−4.168	−9.161	4	$E_4(g_u)$	25	1.494	−3.499	4	$E_{24}(g_u)$
6	−3.854	−8.847	5	$E_7(h_g)$	26	1.808	−3.185	5	$E_{27}(h_g)$
7	−3.794	−8.787	4	$E_6(g_g)$	27	1.868	−3.125	4	$E_{26}(g_g)$
8	−3.530	−8.523	3	$E_8(t_{2u})$	28	2.132	−2.861	3	$E_{28}(t_{2u})$
9	−3.530	−8.523	3	$E_9(t_{1u})$	29	2.132	−2.861	3	$E_{29}(t_{1u})$
10	−3.263	−8.256	5+3	$E_{10,1}(h_u), E_{10,2}(t_{1g})$	30	2.399	−2.594	5+3	$E_{30,1}(h_u), E_{30,2}(t_{1g})$
11	−3.023	−8.016	4	$E_{11}(g_g)$	31	2.639	−2.354	4	$E_{31}(g_g)$
12	−2.332	−7.325	4	$E_{12}(g_u)$	32	3.330	−1.663	4	$E_{32}(g_u)$
13	−2.132	−7.125	5	$E_{13}(h_g)$	33	3.530	−1.463	5	$E_{33}(h_g)$
14	−2.132	−7.125	1	$E_{14}(a_g)$	34	3.530	−1.463	1	$E_{34}(a_g)$
15	−1.992	−6.985	3	$E_{15}(t_{1u})$	35	3.670	−1.323	3	$E_{35}(t_{1u})$
16	−1.699	−6.692	5+3	$E_{16,1}(h_u), E_{16,2}(t_{2g})$	36	3.963	−1.030	5+3	$E_{36,1}(h_u), E_{36,2}(t_{2g})$
17	−1.477	−6.470	5	$E_{17}(h_g)$	37	4.185	−0.808	5	$E_{37}(h_g)$
18	−1.293	−6.286	4	$E_{18}(g_u)$	38	4.369	−0.624	4	$E_{38}(g_u)$
19	−0.977	−5.970	4	$E_{19}(g_g)$	39	4.685	−0.308	4	$E_{39}(g_g)$
20	−0.943	−5.936	3	$E_{20}(t_{2u})$	40	4.719	−0.274	3	$E_{40}(t_{2u})$

The optical absorption spectrum is an essential physical characteristic of a molecule. Using the above energy spectra of endohedral fullerenes $Lu_3N@C_{80}$ and $Y_3N@C_{80}$ with symmetry group I_h, one may determine the transitions that shape the optical spectra of these molecules. The group theory [23] may be used to demonstrate that a molecule with symmetry group I_h has the following allowed transitions in its energy spectrum:

$$\begin{aligned} &t_{1g} \leftrightarrow a_u, \quad t_{1g} \leftrightarrow h_u, \quad t_{1u} \leftrightarrow a_g, \\ &t_{1u} \leftrightarrow t_{1g}, \quad t_{1u} \leftrightarrow h_g, \quad t_{2u} \leftrightarrow g_g, \\ &t_{2u} \leftrightarrow h_g, \quad t_{2g} \leftrightarrow g_u, \quad t_{2g} \leftrightarrow h_u, \\ &g_u \leftrightarrow g_g, \quad g_u \leftrightarrow h_g, \quad g_g \leftrightarrow h_u, \\ &h_g \leftrightarrow h_u. \end{aligned} \tag{16}$$

It follows from the energy spectra of endohedral fullerenes $Lu_3N@C_{80}$ and $Y_3N@C_{80}$ with symmetry group I_h and relations (16) that these molecules have 166 allowed transitions. These transitions are listed in Tables 3 and 4.

The optical absorption spectra of endohedral fullerenes $Lu_3N@C_{80}$ and $Y_3N@C_{80}$ in a toluene solution were obtained in [26]. It was found that the optical absorption spectra of these molecules feature five well-marked absorption bands *a, b, c, d, e* (see Fig. 5). Two of them (*a* and *b*) are fairly intense, while the remaining three low-intensity bands (*c, d*, and *e*) manifest themselves only if the concentration of endohedral fullerenes $Lu_3N@C_{80}$ and $Y_3N@C_{80}$ in the toluene solution is increased. The experimental wavelength and energy values characterizing the absorption bands (letters correspond to the position of these bands in the curves shown in Fig. 5) are listed in Tables 5 and 6. It is also evident from Fig. 5 that the absorption bands of $Lu_3N@C_{80}$ start to form at 807 nm (1.539 eV), while the bands of molecule $Y_3N@C_{80}$ start forming at 786 nm (1.581 eV) [26].

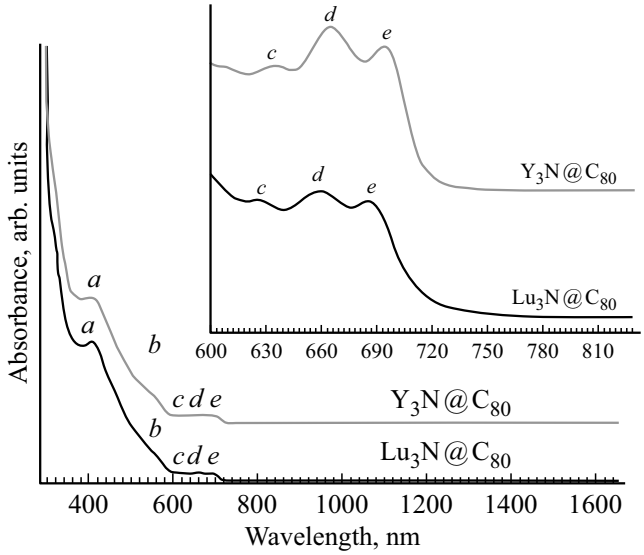

Figure 5. Absorption spectra of $Y_3N@C_{80}$ and $Lu_3N@C_{80}$ in a toluene solution [26]. The absorption spectra corresponding to a higher concentration of $Y_3N@C_{80}$ and $Lu_3N@C_{80}$ in the solution are shown in the inset.

Table 3. Allowed transitions in the energy spectrum of endohedral fullerene $Lu_3N@C_{80}$ with symmetry group I_h

№	ΔE	ΔE, eV	№	ΔE	ΔE, eV	№	ΔE	ΔE, eV	№	ΔE	ΔE, eV
1	$E_{23}-E_{22}$	0.250	43	$E_{31}-E_{16.1}$	4.310	85	$E_{30.2}-E_{10.1}$	5.662	127	$E_{39}-E_{12}$	7.060
2	$E_{27}-E_{22}$	0.980	44	$E_{23}-E_{10.1}$	4.322	86	$E_{40}-E_{19}$	5.697	128	$E_{33}-E_{9}$	7.102
3	$E_{29}-E_{21}$	1.445	45	$E_{30.2}-E_{15}$	4.343	87	$E_{35}-E_{14}$	5.806	129	$E_{29}-E_{1}$	7.107
4	$E_{30.2}-E_{22}$	1.589	46	$E_{25}-E_{11}$	4.370	88	$E_{35}-E_{13}$	5.816	130	$E_{34}-E_{9}$	7.112
5	$E_{23}-E_{20}$	1.934	47	$E_{33}-E_{20}$	4.438	89	$E_{38}-E_{17}$	5.854	131	$E_{33}-E_{8}$	7.117
6	$E_{25}-E_{19}$	2.260	48	$E_{24}-E_{11}$	4.472	90	$E_{33}-E_{12}$	5.871	132	$E_{32}-E_{6}$	7.179
7	$E_{23}-E_{18}$	2.296	49	$E_{30.1}-E_{13}$	4.497	91	$E_{37}-E_{16.1}$	5.901	133	$E_{32}-E_{7}$	7.227
8	$E_{24}-E_{19}$	2.362	50	$E_{23}-E_{9}$	4.598	92	$E_{31}-E_{10.1}$	5.906	134	$E_{30.2}-E_{2}$	7.251
9	$E_{27}-E_{20}$	2.664	51	$E_{23}-E_{8}$	4.613	93	$E_{23}-E_{2}$	5.912	135	$E_{36.2}-E_{10.1}$	7.258
10	$E_{26}-E_{20}$	2.712	52	$E_{32}-E_{17}$	4.784	94	$E_{28}-E_{6}$	5.933	136	$E_{36.1}-E_{10.2}$	7.258
11	$E_{23}-E_{16.1}$	2.726	53	$E_{33}-E_{18}$	4.800	95	$E_{30.2}-E_{9}$	5.937	137	$E_{38}-E_{11}$	7.444
12	$E_{33}-E_{22}$	2.754	54	$E_{36.1}-E_{19}$	4.904	96	$E_{25}-E_{3}$	5.954	138	$E_{37}-E_{10.1}$	7.497
13	$E_{34}-E_{22}$	2.764	55	$E_{31}-E_{12}$	4.950	97	$E_{28}-E_{7}$	5.981	139	$E_{35}-E_{7}$	7.590
14	$E_{25}-E_{17}$	2.780	56	$E_{32}-E_{16.2}$	5.022	98	$E_{39}-E_{18}$	5.989	140	$E_{33}-E_{4}$	7.772
15	$E_{24}-E_{17}$	2.882	57	$E_{27}-E_{10.1}$	5.053	99	$E_{29}-E_{7}$	5.996	141	$E_{37}-E_{9}$	7.772
16	$E_{23}-E_{15}$	3.003	58	$E_{26}-E_{10.1}$	5.101	100	$E_{27}-E_{4}$	5.998	142	$E_{37}-E_{8}$	7.787
17	$E_{28}-E_{19}$	3.018	59	$E_{37}-E_{20}$	5.108	101	$E_{26}-E_{4}$	6.047	143	$E_{40}-E_{11}$	7.807
18	$E_{27}-E_{18}$	3.026	60	$E_{28}-E_{11}$	5.128	102	$E_{24}-E_{3}$	6.056	144	$E_{36.1}-E_{6}$	7.819
19	$E_{35}-E_{21}$	3.039	61	$E_{35}-E_{17}$	5.146	103	$E_{38}-E_{16.2}$	6.092	145	$E_{36.1}-E_{7}$	7.867
20	$E_{30.2}-E_{16.1}$	3.066	62	$E_{25}-E_{6}$	5.175	104	$E_{36.1}-E_{13}$	6.093	146	$E_{33}-E_{5}$	7.875
21	$E_{26}-E_{18}$	3.075	63	$E_{25}-E_{7}$	5.223	105	$E_{27}-E_{5}$	6.101	147	$E_{32}-E_{3}$	7.958
22	$E_{24}-E_{16.2}$	3.120	64	$E_{33}-E_{16.1}$	5.231	106	$E_{26}-E_{5}$	6.149	148	$E_{39}-E_{10.1}$	8.016
23	$E_{30.1}-E_{19}$	3.308	65	$E_{36.2}-E_{18}$	5.232	107	$E_{37}-E_{15}$	6.178	149	$E_{36.2}-E_{4}$	8.204
24	$E_{23}-E_{12}$	3.366	66	$E_{23}-E_{4}$	5.268	108	$E_{31}-E_{8}$	6.196	150	$E_{38}-E_{6}$	8.249
25	$E_{37}-E_{22}$	3.424	67	$E_{24}-E_{6}$	5.277	109	$E_{40}-E_{17}$	6.216	151	$E_{38}-E_{7}$	8.298
26	$E_{25}-E_{13}$	3.449	68	$E_{24}-E_{7}$	5.326	110	$E_{30.1}-E_{6}$	6.223	152	$E_{39}-E_{8}$	8.306
27	$E_{27}-E_{16.1}$	3.457	69	$E_{27}-E_{9}$	5.328	111	$E_{30.1}-E_{7}$	6.271	153	$E_{35}-E_{3}$	8.321
28	$E_{26}-E_{16.1}$	3.505	70	$E_{38}-E_{19}$	5.335	112	$E_{36.2}-E_{12}$	6.302	154	$E_{33}-E_{2}$	8.416
29	$E_{31}-E_{20}$	3.517	71	$E_{27}-E_{8}$	5.343	113	$E_{32}-E_{11}$	6.374	155	$E_{34}-E_{2}$	8.426
30	$E_{28}-E_{17}$	3.537	72	$E_{23}-E_{5}$	5.370	114	$E_{39}-E_{16.1}$	6.420	156	$E_{37}-E_{4}$	8.442
31	$E_{29}-E_{17}$	3.552	73	$E_{29}-E_{10.2}$	5.387	115	$E_{38}-E_{13}$	6.524	157	$E_{37}-E_{5}$	8.544
32	$E_{24}-E_{13}$	3.552	74	$E_{26}-E_{8}$	5.391	116	$E_{37}-E_{12}$	6.540	158	$E_{36.1}-E_{3}$	8.598
33	$E_{27}-E_{15}$	3.734	75	$E_{30.1}-E_{11}$	5.418	117	$E_{27}-E_{2}$	6.642	159	$E_{40}-E_{6}$	8.612
34	$E_{30.1}-E_{17}$	3.827	76	$E_{36.1}-E_{17}$	5.423	118	$E_{28}-E_{3}$	6.711	160	$E_{40}-E_{7}$	8.660
35	$E_{31}-E_{18}$	3.880	77	$E_{32}-E_{13}$	5.453	119	$E_{29}-E_{3}$	6.726	161	$E_{35}-E_{1}$	8.701
36	$E_{30.1}-E_{16.2}$	4.066	78	$E_{37}-E_{18}$	5.470	120	$E_{33}-E_{10.1}$	6.827	162	$E_{39}-E_{4}$	8.962
37	$E_{27}-E_{12}$	4.097	79	$E_{33}-E_{15}$	5.508	121	$E_{31}-E_{4}$	6.852	163	$E_{38}-E_{3}$	9.028
38	$E_{26}-E_{12}$	4.145	80	$E_{34}-E_{15}$	5.518	122	$E_{40}-E_{13}$	6.886	164	$E_{39}-E_{5}$	9.064
39	$E_{28}-E_{13}$	4.207	81	$E_{39}-E_{20}$	5.627	123	$E_{31}-E_{5}$	6.954	165	$E_{37}-E_{2}$	9.086
40	$E_{29}-E_{14}$	4.212	82	$E_{30.1}-E_{10.2}$	5.662	124	$E_{35}-E_{10.2}$	6.981	166	$E_{40}-E_{3}$	9.390
41	$E_{29}-E_{13}$	4.222	83	$E_{36.2}-E_{16.1}$	5.662	125	$E_{30.1}-E_{3}$	7.002			
42	$E_{32}-E_{19}$	4.264	84	$E_{36.1}-E_{16.2}$	5.662	126	$E_{36.1}-E_{11}$	7.014			

Knowing the energy spectra of endohedral fullerenes $Lu_3N@C_{80}$ and $Y_3N@C_{80}$, one may characterize the optical absorption spectra of these molecules in the following way. The optical absorption bands of $Lu_3N@C_{80}$ and $Y_3N@C_{80}$ corresponding to energies $E_a, E_b, E_c, E_d, and E_e$ in Fig. 5 may be interpreted as bands formed by the following transitions:

for the $Lu_3N@C_{80}$ molecule

$$E_a = E_{26} - E_{18},\ E_b = E_{25} - E_{19},\ E_c = E_{23} - E_{19},$$

$$E_c = E_{31} - E_{21},\ E_d = E_{23} - E_{20},\ E_e = E_{31} - E_{22}, \quad (17)$$

for the $Y_3N@C_{80}$ molecule

$$E_a = E_{23} - E_{15},\ E_b = E_{25} - E_{19},\ E_c = E_{23} - E_{20},$$

$$E_d = E_{31} - E_{21},\ E_e = E_{31} - E_{22}. \quad (18)$$

The numerical values of energies corresponding to E_a, E_b, E_c, E_d, E_e from (17) and (18) are listed in Tables 5 and 6. It can be seen from these tables that the theoretical values of energies are close to the experimental ones [26]. Note that energies E_a, E_b, E_d for the $Lu_3N@C_{80}$ molecule correspond to allowed transitions, while energies E_c, E_e correspond to forbidden transitions. In the case

Table 4. Allowed transitions in the energy spectrum of endohedral fullerene $Y_3N@C_{80}$ with symmetry group I_h

№	ΔE	ΔE, eV	№	ΔE	ΔE, eV	№	ΔE	ΔE, eV	№	ΔE	ΔE, eV
1	$E_{23}-E_{22}$	0.241	43	$E_{31}-E_{16.1}$	4.338	85	$E_{30.2}-E_{10.1}$	5.662	127	$E_{39}-E_{12}$	7.017
2	$E_{27}-E_{22}$	0.948	44	$E_{23}-E_{10.1}$	4.364	86	$E_{40}-E_{19}$	5.696	128	$E_{33}-E_{9}$	7.060
3	$E_{29}-E_{21}$	1.399	45	$E_{30.2}-E_{15}$	4.391	87	$E_{35}-E_{14}$	5.802	129	$E_{34}-E_{9}$	7.060
4	$E_{30.2}-E_{22}$	1.539	46	$E_{25}-E_{11}$	4.397	88	$E_{35}-E_{13}$	5.802	130	$E_{29}-E_{1}$	7.061
5	$E_{23}-E_{20}$	2.044	47	$E_{33}-E_{20}$	4.473	89	$E_{38}-E_{17}$	5.846	131	$E_{33}-E_{8}$	7.092
6	$E_{25}-E_{19}$	2.351	48	$E_{24}-E_{11}$	4.517	90	$E_{33}-E_{12}$	5.862	132	$E_{32}-E_{6}$	7.124
7	$E_{23}-E_{18}$	2.394	49	$E_{30.1}-E_{13}$	4.531	91	$E_{37}-E_{16.1}$	5.884	133	$E_{32}-E_{7}$	7.184
8	$E_{24}-E_{19}$	2.471	50	$E_{23}-E_{9}$	4.631	92	$E_{31}-E_{10.1}$	5.902	134	$E_{30.2}-E_{2}$	7.201
9	$E_{33}-E_{22}$	2.670	51	$E_{23}-E_{8}$	4.663	93	$E_{23}-E_{2}$	5.903	135	$E_{36.2}-E_{10.1}$	7.226
10	$E_{34}-E_{22}$	2.670	52	$E_{32}-E_{17}$	4.807	94	$E_{28}-E_{6}$	5.926	136	$E_{36.1}-E_{10.2}$	7.226
11	$E_{27}-E_{20}$	2.751	53	$E_{33}-E_{18}$	4.823	95	$E_{30.2}-E_{9}$	5.929	137	$E_{38}-E_{11}$	7.392
12	$E_{23}-E_{16.1}$	2.800	54	$E_{36.1}-E_{19}$	4.940	96	$E_{25}-E_{3}$	5.935	138	$E_{37}-E_{10.1}$	7.448
13	$E_{26}-E_{20}$	2.811	55	$E_{31}-E_{12}$	4.971	97	$E_{28}-E_{7}$	5.986	139	$E_{35}-E_{7}$	7.524
14	$E_{25}-E_{17}$	2.851	56	$E_{32}-E_{16.2}$	5.029	98	$E_{27}-E_{4}$	5.976	140	$E_{33}-E_{4}$	7.698
15	$E_{35}-E_{21}$	2.937	57	$E_{27}-E_{10.1}$	5.071	99	$E_{39}-E_{18}$	5.978	141	$E_{37}-E_{9}$	7.715
16	$E_{24}-E_{17}$	2.971	58	$E_{37}-E_{20}$	5.128	100	$E_{29}-E_{7}$	5.986	142	$E_{40}-E_{11}$	7.742
17	$E_{23}-E_{15}$	3.093	59	$E_{26}-E_{10.1}$	5.131	101	$E_{26}-E_{4}$	6.036	143	$E_{37}-E_{8}$	7.747
18	$E_{27}-E_{18}$	3.101	60	$E_{35}-E_{17}$	5.147	102	$E_{24}-E_{3}$	6.055	144	$E_{36.1}-E_{6}$	7.757
19	$E_{28}-E_{19}$	3.109	61	$E_{28}-E_{11}$	5.155	103	$E_{38}-E_{16.2}$	6.068	145	$E_{36.1}-E_{7}$	7.817
20	$E_{26}-E_{18}$	3.161	62	$E_{25}-E_{6}$	5.168	104	$E_{36.1}-E_{13}$	6.095	146	$E_{33}-E_{5}$	7.817
21	$E_{24}-E_{16.2}$	3.193	63	$E_{25}-E_{7}$	5.228	105	$E_{27}-E_{5}$	6.095	147	$E_{32}-E_{3}$	7.891
22	$E_{37}-E_{22}$	3.325	64	$E_{33}-E_{16.1}$	5.229	106	$E_{26}-E_{5}$	6.155	148	$E_{39}-E_{10.1}$	7.948
23	$E_{30.1}-E_{19}$	3.376	65	$E_{36.2}-E_{18}$	5.256	107	$E_{37}-E_{15}$	6.177	149	$E_{36.2}-E_{4}$	8.131
24	$E_{23}-E_{12}$	3.433	66	$E_{23}-E_{4}$	5.269	108	$E_{30.1}-E_{6}$	6.193	150	$E_{38}-E_{6}$	8.163
25	$E_{25}-E_{13}$	3.506	67	$E_{24}-E_{6}$	5.288	109	$E_{40}-E_{17}$	6.196	151	$E_{38}-E_{7}$	8.223
26	$E_{27}-E_{16.1}$	3.507	68	$E_{27}-E_{9}$	5.338	110	$E_{31}-E_{8}$	6.201	152	$E_{35}-E_{3}$	8.231
27	$E_{26}-E_{16.1}$	3.567	69	$E_{38}-E_{19}$	5.346	111	$E_{30.1}-E_{7}$	6.253	153	$E_{34}-E_{2}$	8.332
28	$E_{31}-E_{20}$	3.582	70	$E_{24}-E_{7}$	5.348	112	$E_{36.2}-E_{12}$	6.295	154	$E_{33}-E_{2}$	8.332
29	$E_{28}-E_{17}$	3.609	71	$E_{27}-E_{8}$	5.370	113	$E_{32}-E_{11}$	6.353	155	$E_{39}-E_{8}$	8.247
30	$E_{29}-E_{17}$	3.609	72	$E_{23}-E_{5}$	5.388	114	$E_{39}-E_{16.1}$	6.384	156	$E_{37}-E_{4}$	8.353
31	$E_{24}-E_{13}$	3.626	73	$E_{29}-E_{10.2}$	5.395	115	$E_{38}-E_{13}$	6.501	157	$E_{37}-E_{5}$	8.472
32	$E_{27}-E_{15}$	3.800	74	$E_{26}-E_{8}$	5.430	116	$E_{37}-E_{12}$	6.517	158	$E_{40}-E_{6}$	8.513
33	$E_{30.1}-E_{17}$	3.876	75	$E_{36.1}-E_{17}$	5.440	117	$E_{27}-E_{2}$	6.610	159	$E_{36.1}-E_{3}$	8.524
34	$E_{31}-E_{18}$	3.932	76	$E_{30.1}-E_{11}$	5.422	118	$E_{28}-E_{3}$	6.693	160	$E_{40}-E_{7}$	8.573
35	$E_{30.2}-E_{16.1}$	4.098	77	$E_{32}-E_{13}$	5.462	119	$E_{29}-E_{3}$	6.693	161	$E_{35}-E_{1}$	8.599
36	$E_{30.1}-E_{16.2}$	4.098	78	$E_{37}-E_{18}$	5.478	120	$E_{33}-E_{10.1}$	6.793	162	$E_{39}-E_{4}$	8.853
37	$E_{27}-E_{12}$	4.200	79	$E_{33}-E_{15}$	5.522	121	$E_{31}-E_{4}$	6.807	163	$E_{38}-E_{3}$	8.930
38	$E_{26}-E_{12}$	4.200	80	$E_{34}-E_{15}$	5.522	122	$E_{40}-E_{13}$	6.851	164	$E_{39}-E_{5}$	8.972
39	$E_{28}-E_{13}$	4.264	81	$E_{39}-E_{20}$	5.628	123	$E_{31}-E_{5}$	6.926	165	$E_{37}-E_{2}$	8.987
40	$E_{29}-E_{14}$	4.264	82	$E_{30.1}-E_{10.2}$	5.662	124	$E_{35}-E_{10.2}$	6.933	166	$E_{40}-E_{3}$	9.280
41	$E_{29}-E_{13}$	4.264	83	$E_{36.2}-E_{16.1}$	5.662	125	$E_{30.1}-E_{3}$	6.960			
42	$E_{32}-E_{19}$	4.307	84	$E_{36.1}-E_{16.2}$	5.662	126	$E_{36.1}-E_{11}$	6.986			

Table 5. Experimental and theoretical wavelength and energy values corresponding to the absorption bands in the optical spectrum of $Lu_3N@C_{80}$

Parameter	*a*	*b*	*c*	*d*	*e*
λ, nm [26]	403	548	626	658	685
E, eV [26]	3.083	2.267	1.985	1.888	1.814
E, eV, theory	3.075	2.260	1.965;1.968	1.934	1.833

Table 6. Experimental and theoretical wavelength and energy values corresponding to the absorption bands in the optical spectrum of $Y_3N@C_{80}$

Parameter	*a*	*b*	*c*	*d*	*e*
λ, nm [26]	407	549	633	665	694
E, eV [26]	3.053	2.263	1.963	1.868	1.790
E, eV, theory	3.093	2.351	2.044	1.906	1.779

of $Y_3N@C_{80}$, energies E_a, E_b, E_c correspond to allowed transitions, while energies E_d, E_e correspond to forbidden transitions. Forbidden transitions may manifest themselves as a result of symmetry violation occurring due to the fact that atoms in a molecule undergo small-amplitude oscillations about the equilibrium position. Owing to symmetry violation, symmetry-forbidden optical transitions become allowed with a low intensity. This is the reason why forbidden transitions form absorption bands with a very low intensity.

4. Conclusion

Thus, the experimentally observed optical absorption spectra of endohedral fullerenes $Lu_3N@C_{80}$ and $Y_3N@C_{80}$ agree fairly closely with the optical absorption spectra of these molecules derived from the energy spectra of $Lu_3N@C_{80}$ and $Y_3N@C_{80}$ within the Hubbard model in the static fluctuation approximation.

Note that the energy spectra of fullerenes C_{60} and C_{70} studied in [17,18] were also determined within the Hubbard model in the static fluctuation approximation. These studies revealed that the experimental optical absorption spectra of C_{60} and C_{70} also agree fairly well with the optical absorption spectra of these molecules derived within the Hubbard model in the static fluctuation approximation. This allows one to state that the Hubbard model in the static fluctuation approximation characterizes quite well the electronic properties of carbon nanosystems.

Conflict of interest

The author declares that he has no conflict of interest.

References

[1] H.W. Kroto, J.R. Heath, S.C. O'Brien, R.F. Curl, R.E. Smalley. Nature **318**, 162 (1985).
[2] H.W. Kroto. Nature **329**, 529 (1987).
[3] M. Krause, J. Wong, L. Dunsch. Chem. Eur. J. **11**, 706 (2005).
[4] S. Yang, L. Dunsch. J. Phys. Chem. B **109**, 12320 (2005).
[5] S. Stevenson, H.M. Lee, M.M. Olmstead, C. Kozikowski, P. Stevenson, A.L. Balch. Chem. Eur. J. **8**, *19*, 4528 (2002).
[6] L. Echegoyen, C.J. Chancellor, C.M. Cardona, B. Elliott, J. Rivera, M.M. Olmstead, A.L. Balch. Chem. Commun. 2653 (2006).
[7] P.W. Fowler, D.E. Manolopoulous. An atlas of fullerenes. Clarendon, Oxford (1995).
[8] O.E. Glukhova, A.I. Zhbanov, A.G. Rezkov. Phys. Solid State **47**, *2*, 390 (2005).
[9] J. Ding, S. Yang. Angew. Chem. Int. Ed. **35**, 2234 (1996).
[10] J.C. Duchamp, A. Demortier, K.R. Fletcher, D. Dorn, E.B. Iezzi, T. Glass, H.C. Dorn. Chem. Phys. Lett. **375**, 655 (2003).
[11] J. Hubbard. Proc. Roy. Soc. London A **276**, 238 (1963).
[12] A.V. Silant'ev. Phys. Solid State **61**, *2*, 263 (2019).
[13] A.V. Silant'ev. Phys. Solid State **62**, *3*, 542 (2020).
[14] A.V. Silant'ev. Phys. Solid State **63**, *11*, 225 (2021).
[15] A.V. Silant'ev. Phys. Solid State **62**, *11*, 2208 (2020).
[16] A.V. Silant'ev. Russ. Phys. J. **62**, *6*, 925 (2019).
[17] A.V. Silant'ev. J. Exp. Theor. Phys. **121**, 653 (2015).
[18] A.V. Silant'ev. Russ. Phys. J. **60**, *6*, 978 (2017).
[19] G.S. Ivanchenko, N.G. Lebedev. Phys. Solid State **49**, 189 (2007).
[20] A.V. Silant'ev. Russ. Phys. J. **56**, *2*, 192 (2013).
[21] A.V. Eletskii. Phys.-Usp. **43**, *2*, 111 (2000).
[22] S.V. Tyablikov. Methods in the Quantum Theory of Magnetism (Nauka, Moscow, 1975; Plenum, New York, 1967).
[23] R.M. Hochstrasser. Molecular Aspects of Symmetry. W. A. Benjamin. (1966).
[24] R.A. Harris, L.M. Falicov. J. Chem. Phys. **51**, 5034 (1969).
[25] L. Basurto, F. Amerikheirabadi, R. Zope, T. Baruah. J. Phys. Chem. Chem. Phys. **17**, 5832 (2015).
[26] S. Yang, A.A. Popov, L. Dunsch. Angew. Chem. Int. Ed. **47**, 8196 (2008).